FACILITATED PERTRACTION OF INDOLE 3-ACETIC ACID IN THE PRESENCE OF TRIOCTYLAMINE AS A CARRIER

Sorina Laura TOPALĂ[1], Ioana DIACONU[2*], Oana Cristina PÂRVULESCU[3*], Roxana Sânziana JIDVEIAN[4], Ana Maria DRĂGHICI-POPA[5]

The transfer of indole 3-acetic acid (IAA) from a feed (F) phase (an aqueous solution of IAA) to a stripping (S) phase (an aqueous solution of NaOH), using a chloroform liquid membrane (M) and trioctylamine (TOA) as a carrier, was studied at different levels of pertraction process factors, i.e., initial molar concentrations of IAA in the F phase ($c_{IAA,F0}$ = 10^{-4}–10^{-3} kmol/m^3) and NaOH in the S phase ($c_{NaOH,S0}$ = 10^{-2}–1 kmol/m^3). Each experiment was performed for 4 h, at 20 °C, at an initial molar concentration of TOA in the M phase of 10^{-2} kmol/m^3, in a tube-in-tube device, under mechanical stirring of inner tube (200 rpm). The inner tube contained the S phase, and the outer tube contained the F phase at the top and the M phase at the bottom. Specific yields of IAA in the F, M, and S phases were predicted based on a kinetic model assuming consecutive irreversible first-order reactions. The values of extraction and stripping rate constants, i.e., k_1 = (1.93–3.64)×10^{-4} s^{-1} and k_2 = (2.00–4.18)×10^{-4} s^{-1}, were similar, indicating that both chemical reactions occurring at the interfaces between the F and M phases (complexation) and M and S phases (decomplexation) were rate-limiting steps. The maximum experimental value of recovery efficiency of IAA (91.09%) was obtained at $c_{IAA,F0}$ = 10^{-4} kmol/m^3 and $c_{NaOH,S0}$ = 1 kmol/m^3.

Keywords: indole 3-acetic acid (IAA), liquid membrane, kinetic model, mass transfer, pertraction, trioctylamine (TOA)

1. Introduction

Indole 3-acetic acid (IAA) is an important phytohormone from the auxin class. It plays a key role in plant germination, growth, and development, being involved in cell division, elongation, and differentiation [1–5]. Positive effects on the plant height, root and shoot development, number of branches, leaves, flowers, pods, fruits, and seeds were reported for plants treated with IAA [1,3,6,7].

[1] Ph.D. Student, Dept. of Chemical and Biochemical Engineering, NUST POLITEHNICA Bucharest, Romania
[2*] Assoc. Prof., Dept. of Analytical Chemistry and Environmental Engineering, NUST POLITEHNICA Bucharest, Romania, e-mail: ioana.diaconu@upb.ro (corresponding author)
[3*] Prof., Dept. of Chemical and Biochemical Engineering, NUST POLITEHNICA Bucharest, Romania, e-mail: oana.parvulescu@upb.ro, oana.parvulescu@yahoo.com (corresponding author)
[4] Ph.D. Student, Dept. of Chemical and Biochemical Engineering, NUST POLITEHNICA Bucharest, Romania
[5] Ph.D. Student, Dept. of Organic Chemistry, NUST POLITEHNICA Bucharest, Romania

Moreover, IAA application often enhances the plant resistance to abiotic stresses, *e.g.*, drought, extreme temperatures, salinity, heavy metal toxicity [1,5,8]. Biostimulants and biofertilizers based on IAA could lead to significant environmental and agronomic benefits [1].

IAA can be obtained by extraction from plants and chemical or microbial synthesis. It is synthesized by various bacteria (*e.g.*, from genus *Alcaligenes*, *Azospirillum*, *Azotobacter*, *Bacillus*, *Enterobacter*, *Klebsiella*, *Pantoea*, *Pseudomonas*, *Rhizobium*, *Streptomyces*), fungi (*e.g.*, from genus *Amanita*, *Colletotrichum*, *Laccaria*, *Paxillus*, *Phytophthora*, *Pisolithus*, *Rhizopogon*, *Taphrina*, *Ustilago*, *Absidia*, *Aspergillus*, *Fusarium*, *Penicillium*, *Rhizoctonia*, *Rhizopus*), and yeasts (*e.g.*, from genus *Aureobasidium*, *Candida*, *Debaryomyces*, *Filobasidium*, *Hanseniaspora*, *Metschnikowia*, *Meyerozyma*, *Paenibacillus*, *Rhodotorula*, *Yarrowia*) [1,2,3,6,9,10].

Facilitated pertraction is a rapid, inexpensive, and effective technique used for the selective separation and concentration of IAA and other solutes from dilute aqueous solutions [11–15]. It consists in the mass transfer of a solute from an aqueous solution, *i.e.*, feed (F) phase, to another aqueous solution, *i.e.*, stripping (S) phase, using a liquid membrane (M) phase, consisting of an organic solvent and a suitable carrier [13,14]. This process involves the following steps: (i) complexation reaction between the solute and carrier at the interface between the F and M phases; (ii) diffusion of the solute-carrier complex (CX) through the M phase; (iii) decomplexation reaction between the CX and stripping agent at the interface between the M and S phases, resulting in the release of the solute in the S phase and the carrier in the M phase [16–20]. The solute recovery efficiency can be strongly influenced by the process factors, especially the type of solute, membrane, carrier, and stripping agent, initial composition and volumes of F, M, and S phases, type and dimensions of the separation device.

In this paper, an experimental study and modelling of the separation of IAA from a dilute aqueous solution using chloroform as an organic solvent in the M phase and trioctylamine (TOA) as a carrier were presented. The effects of the process factors, *i.e.*, initial concentrations of IAA in the F phase (10^{-4}–10^{-3} kmol/m^3) and NaOH (stripping agent) in the S phase (10^{-2}–1 kmol/m^3), on its performances were evaluated.

2. Materials and methods

IAA, chloroform, TOA, and NaOH were analytical grade reagents purchased from LiChrosolv® (Merck, Germany).

The membrane system consisted of the following components: (i) F phase – IAA aqueous solution; (ii) M phase – chloroform + TOA; (iii) S phase – NaOH aqueous solution. For the preparation of F and S phases, distilled water (DW)

saturated with chloroform was used, and for the preparation of M phase, chloroform saturated with DW was used.

The mass transfer of IAA species from F phase to S phase was conducted in a tube-in-tube device [11,12]. The F and M phases were placed at the top and bottom, respectively, of the outer glass tube. The S phase was placed in the inner glass tube, which was continuously stirred (ν = 200 rpm). More information on the experimental setup and mass transfer process is given in our previous papers [11,12].

Facilitated pertraction experiments were carried out at different levels of initial molar concentrations of IAA and NaOH in the F and S phases, namely $c_{IAA,F0}$ = 10^{-4}–10^{-3} kmol/m^3 and $c_{NaOH,S0}$ = 10^{-2}–1 kmol/m^3. Each experiment was performed for 4 h, at 20 °C, and at an initial molar concentration of carrier (ligand) in the M phase ($c_{L,M0}$) of 10^{-2} kmol/m^3. It was assumed that the liquid phases were perfectly mixed and their volumes remained constant during the transfer process (V_F = 20×10^{-6} m^3, V_M = 50×10^{-6} m^3, and V_S = 7×10^{-6} m^3).

The molar concentrations of IAA in the F and S phases at a time t, *i.e.*, $c_{IAA,F}(t)$ and $c_{IAA,S}(t)$, were measured using a spectrophotometer (UV1900i, Shimadzu, Kyoto, Japan), whereas the molar concentration of IAA in the M phase at a time t, *i.e.*, $c_{IAA,M}(t)$, was calculated using equation (1) based on the mass balance of IAA species in the membrane system. Specific amounts of IAA in the F, M, and S phases at a time t, namely $R_F(t)$, $R_M(t)$, and $R_S(t)$, are defined by equations (2)–(4). Equation (5) was obtained by substituting equations (2)–(4) into equation (1).

$$c_{IAA,M}(t)V_M = c_{IAA,F0}V_F - c_{IAA,F}(t)V_F - c_{IAA,S}(t)V_S \tag{1}$$

$$R_F(t) = \frac{c_{IAA,F}(t)V_F}{c_{IAA,F0}V_F} = \frac{c_{IAA,F}(t)}{c_{IAA,F0}} \tag{2}$$

$$R_M(t) = \frac{c_{IAA,M}(t)V_M}{c_{IAA,F0}V_F} \tag{3}$$

$$R_S(t) = \frac{c_{IAA,S}(t)V_S}{c_{IAA,F0}V_F} \tag{4}$$

$$R_F(t) + R_M(t) + R_S(t) = 1 \tag{5}$$

3. Modelling

A kinetic model based on consecutive irreversible first-order reactions, as shown in scheme (6), and characterized by equations (7)–(9), where k_1 and k_2 are the rate constants, was selected to describe the mass transfer process of IAA species in the membrane system. Time variations of specific amounts of IAA in the F, M and S phases are given by equations (10)–(12). Equations (10) and (11) were

obtained by integrating equations (7) and (8), whereas equation (12) resulted by substituting equations (10) and (11) into equation (5).

$$\mathrm{IAA}_{FP} \xrightarrow{k_1} \mathrm{IAA}_{M} \xrightarrow{k_2} \mathrm{IAA}_{SP} \tag{6}$$

$$\frac{dR_F(t)}{dt} = -k_1 R_F(t) \tag{7}$$

$$\frac{dR_M(t)}{dt} = k_1 R_F(t) - k_2 R_M(t) \tag{8}$$

$$\frac{dR_S(t)}{dt} = k_2 R_M(t) \tag{9}$$

$$R_F(t) = e^{-k_1 t} \tag{10}$$

$$R_M(t) = \frac{k_1}{k_2 - k_1}\left(e^{-k_1 t} - e^{-k_2 t}\right) \tag{11}$$

$$R_S(t) = 1 - R_F(t) - R_M(t) = 1 - \frac{1}{k_2 - k_1}\left(k_2 e^{-k_1 t} - k_1 e^{-k_2 t}\right) \tag{12}$$

The maximum value of function $R_M(t)$ given by equation (11), *i.e.*, $R_{M,\max}(t_{\max})$, and the corresponding level of t, *i.e.*, $t_{\max}$, are expressed by equations (13) and (14) [11].

$$R_{M,\max}(t_{\max}) = \left(\frac{k_1}{k_2}\right)^{-\frac{k_2}{k_1 - k_2}} \tag{13}$$

$$t_{\max} = \frac{\ln\left(\frac{k_1}{k_2}\right)}{k_1 - k_2} \tag{14}$$

The kinetic constants k_1 and k_2 were determined from the experimental data using the Excel Solver. The extraction rate constant k_1 was calculated by minimizing the sum of squared residuals SSR_1 defined by equation (15), where $R_{F,ex}(t_i)$ and $R_{F,pred}(t_i)$ are the experimental and predicted values of specific amount of IAA in the F phase at $t_i = 1800i$ ($i = 0, 1\ldots8$). The stripping rate constant k_2 was determined by minimizing the sum of squared residuals SSR_2 given by equation (16), where $R_{S,ex}(t_i)$ and $R_{S,pred}(t_i)$ are the experimental and predicted values of specific amount of IAA in the S phase at t_i.

$$SSR_1 = \sum_{i=0}^{8}\left[R_{F,ex}(t_i) - R_{F,pred}(t_i)\right]^2 \tag{15}$$

$$SSR_2 = \sum_{i=0}^{8}\left[R_{S,ex}(t_i) - R_{S,pred}(t_i)\right]^2 \tag{16}$$

Final values (at t_f = 4 h = 14400 s) of extraction, stripping, and recovery efficiencies of IAA, *i.e.*, E_{Ef}, E_{Sf}, and E_{Rf}, are given by equations (17)–(19), where $c_{IAA,Ff}$, $c_{IAA,Sf}$, R_{Ff}, and R_{Sf} are the final values of molar concentrations and specific amounts of IAA, respectively, in the F and S phases [11].

$$E_{Ef} = 100\left(1 - \frac{c_{IAA,Ff}}{c_{IAA,F0}}\right) = 100\left(1 - R_{Ff}\right) \tag{17}$$

$$E_{Sf} = \frac{100c_{IAA,Sf}V_S}{(c_{IAA,F0} - R_{Ff}c_{IAA,F0})V_F} = \frac{100c_{IAA,Sf}V_S}{(1-R_{Ff})c_{IAA,F0}V_F} = \frac{100R_{Sf}}{1-R_{Ff}} = 10000\frac{R_{Sf}}{E_{Ef}} \tag{18}$$

$$E_{Rf} = 100\frac{c_{IAA,Sf}V_S}{c_{IAA,F0}V_F} = 100R_{Sf} = \frac{E_{Ef}E_{Sf}}{100} \tag{19}$$

4. Results and discussion

Time variation of experimental and predicted values of specific amounts of IAA in the phases of the membrane system at different levels of $c_{IAA,F0}$ and $c_{NaOH,S0}$ are shown in Fig. 1, where $R_{F,pred}$, $R_{M,pred}$, and $R_{S,pred}$ were determined using equations (10)–(12). Characteristic parameters of equations (10)–(12), *i.e.*, k_1, k_2, t_{max} and $R_{M,max}$, are specified in Tables 1 and 2, which also contain the values of sum of squared residuals (SSR_1 and SSR_2), total sum of squares [SST_1 and SST_2 given by equations (20) and (21)], and coefficient of determination (R_1^2 and R_2^2 defined by equations (22) and (23)].

$$SST_1 = \sum_{i=0}^{8}\left[R_{F,ex}(t_i) - \frac{\sum_{i=0}^{8}R_{F,ex}(t_i)}{9}\right]^2 \tag{20}$$

$$SST_2 = \sum_{i=0}^{8}\left[R_{S,ex}(t_i) - \frac{\sum_{i=0}^{8}R_{S,ex}(t_i)}{9}\right]^2 \tag{21}$$

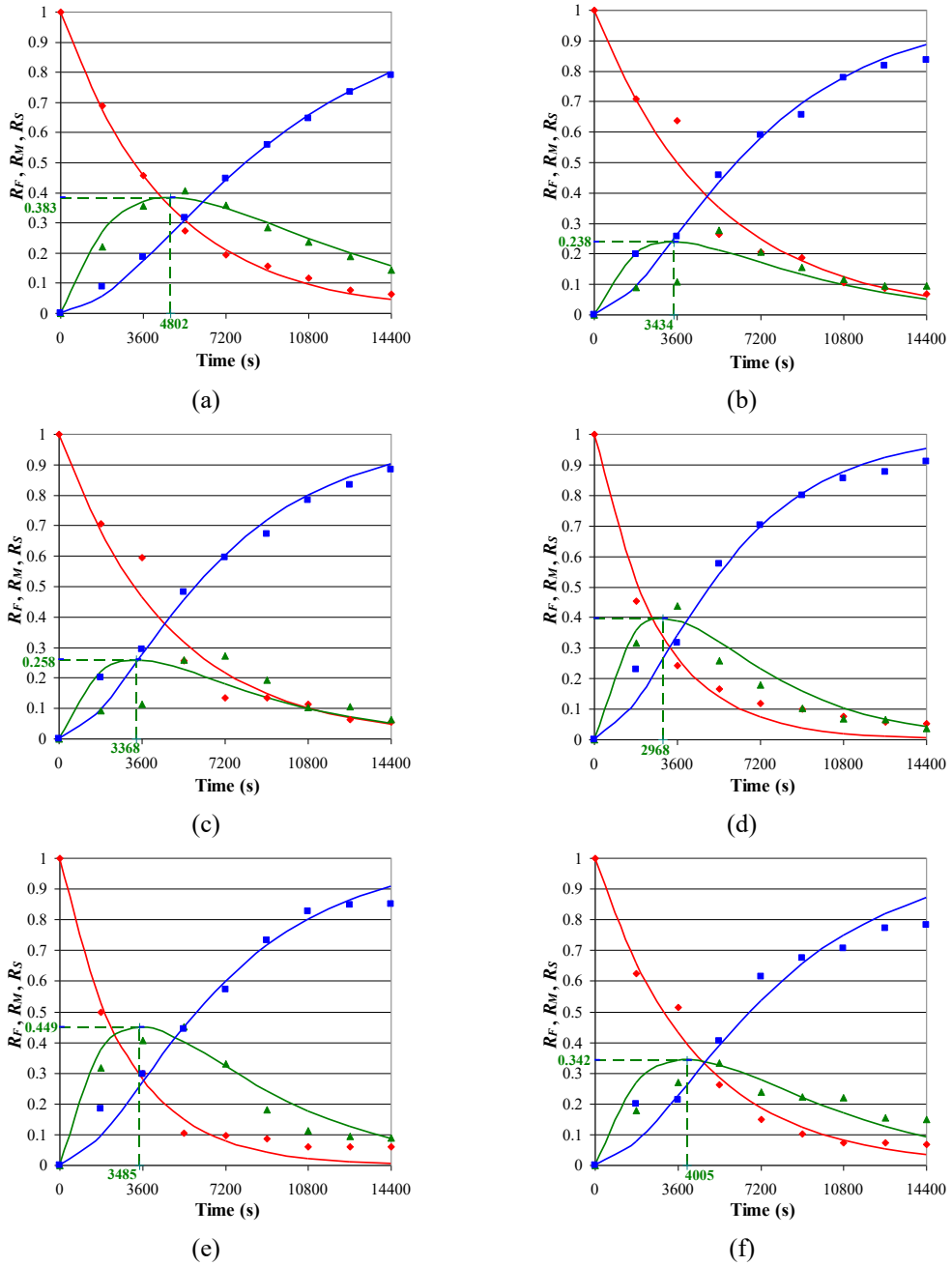

Fig. 1. Effects of initial concentration of IAA in the feed (F) phase ($c_{IAA,F0}$) and initial concentration of NaOH in the stripping (S) phase ($c_{NaOH,S0}$) on dynamics of experimental (bullets) and predicted (lines) specific amounts of IAA in the F (red), liquid membrane (green), and S (blue) phases ($c_{L,M0} = 10^{-2}$ kmol/m^3, $v = 200$ rpm, and $t_f = 4$ h = 14400 s): (a) $c_{IAA,F0} = 10^{-3}$ kmol/m^3 and $c_{NaOH,S0} = 1$ kmol/m^3; (b) $c_{IAA,F0} = 6\times10^{-4}$ kmol/m^3 and $c_{NaOH,S0} = 1$ kmol/m^3; (c) $c_{IAA,F0} = 3\times10^{-4}$ kmol/m^3 and $c_{NaOH,S0} = 1$ kmol/m^3; (d) $c_{IAA,F0} = 10^{-4}$ kmol/m^3 and $c_{NaOH,S0} = 1$ kmol/m^3; (e) $c_{IAA,F0} = 10^{-4}$ kmol/m^3 and $c_{NaOH,S0} = 10^{-1}$ kmol/m^3; (f) $c_{IAA,F0} = 10^{-4}$ kmol/m^3 and $c_{NaOH,S0} = 10^{-2}$ kmol/m^3.

$$R_1^2 = 1 - \frac{SSR_1}{SST_1} \tag{22}$$

$$R_2^2 = 1 - \frac{SSR_2}{SST_2} \tag{23}$$

Table 1

Relevant parameters of data given in Fig. 1a–d ($c_{NaOH,S0}$ = 1 kmol/m^3).

$c_{IAA,F0}$ (kmol/m^3) / Parameter	10^{-4}	3×10^{-4}	6×10^{-4}	10^{-3}
SSR_1	0.019	0.028	0.029	0.003
SST_1	0.757	0.935	0.896	0.825
R_1^2	0.975	0.970	0.967	0.996
$k_1\times10^4$ (s^{-1})	3.64	2.12	1.93	2.17
SSR_2	0.018	0.016	0.017	0.002
SST_2	0.863	0.752	0.724	0.658
R_2^2	0.980	0.979	0.977	0.998
$k_2\times10^4$ (s^{-1})	3.12	4.02	4.18	2.00
$R_{M,\max}$	0.397	0.258	0.238	0.383
$t_{\max}$ (s)	2968	3368	3434	4802

Table 2

Relevant parameters of data given in Fig. 1d–f ($c_{IAA,F0}$ = 10^{-4} kmol/m^3).

$c_{NaOH,S0}$ (kmol/m^3) / Parameter	10^{-2}	10^{-1}	1
SSR_1	0.012	0.012	0.019
SST_1	0.858	0.807	0.757
R_1^2	0.986	0.985	0.975
$k_1\times10^4$ (s^{-1})	2.32	3.53	3.64
SSR_2	0.035	0.014	0.018
SST_2	0.669	0.798	0.863
R_2^2	0.948	0.983	0.980
$k_2\times10^4$ (s^{-1})	2.68	2.30	3.12
$R_{M,\max}$	0.342	0.449	0.397
$t_{\max}$ (s)	4005	3485	2968

Tabulated results highlight a very good agreement between experimental and predicted data (R_1^2 = 0.967–0.996 and R_2^2 = 0.948–0.998). The extraction and stripping rate constants, $k_1 = (1.93–3.64)\times10^{-4}$ s^{-1} and $k_2 = (2.00–4.18)\times10^{-4}$ s^{-1}, were similar, indicating that both reactions occurring at the interfaces between the F and M phases (R1) and M and S phases (R2) were rate-limiting steps in the mass transfer of IAA.

The values of k_1 were lower than those obtained in a previous study performed at the same levels of $c_{IAA,F0}$ and $c_{NaOH,S0}$, but using tributylphosphate (TBF) and trioctylphosphine oxide (TOPO) as carriers, *i.e.*, $k_1 = (5.12–11.35)\times10^{-4}$ s^{-1}, whereas the values of k_2 were generally higher than those reported for TBF and TOPO, *i.e.*, $k_2 = (1.16–2.41)\times10^{-4}$ s^{-1} [15]. Moreover, t_{max} increased with an increase in $c_{IAA,F0}$ and a decrease in $c_{NaOH,S0}$.

$$(H\text{-}A)_F + ((C_8H_{17})_3N)_M \rightleftharpoons ((C_8H_{17})_3NHA)_M \quad (R1)$$

$$((C_8H_{17})_3NHA)_M + (HO^-)_S \rightleftharpoons ((C_8H_{17})_3N)_M + (H_2O)_S + (A^-)_S \quad (R2)$$

The effects of $c_{IAA,F0}$ (10^{-4}–10^{-3} kmol/m^3) and $c_{NaOH,S0}$ (10^{-2}–1 kmol/m^3) on $R_{Ff,ex}$, $R_{Mf,ex}$, $R_{Sf,ex}$, $E_{Ef,ex}$, $E_{Sf,ex}$, and $E_{Rf,ex}$ ($c_{L,M0} = 10^{-2}$ kmol/m^3, v = 200 rpm, and t_f = 4 h) are shown in Figs. 2 and 3. The maximum value of $R_{Sf,ex}$ ($R_{Sf,ex,max}$ = 0.911), corresponding to maximum values of $E_{Ef,ex}$ (94.81%), $E_{Sf,ex}$ (96.08%), and $E_{Rf,ex}$ (91.09%), was obtained at the minimum level of $c_{IAA,F0}$ (10^{-4} kmol/m^3) and maximum level of $c_{NaOH,S0}$ (1 kmol/m^3).

The values of $R_{Sf,ex}$ for the other levels of $c_{IAA,F0}$ (3×10^{-4}–10^{-3} kmol/m^3), *i.e.*, 0.790–0.882, were 3–15% lower than $R_{Sf,ex,max}$ = 0.911 (Fig. 2a). An increase in $c_{IAA,F0}$ (from 10^{-4} kmol/m^3 to 10^{-3} kmol/m^3) had a negative effect on $E_{Sf,ex}$ and $E_{Rf,ex}$ (which decreased from 96.08% to 84.54% and from 91.09% to 79.04%, respectively), but a negligible effect on $E_{Ef,ex}$ (93.17–94.81%) (Fig. 2b). These findings were similar to those reported in our previous study [11].

The values of $R_{Sf,ex}$ for the other levels of $c_{NaOH,S0}$ (10^{-2} kmol/m^3 and 10^{-1} kmol/m^3), *i.e.*, 0.781 and 0.851, were significantly lower (7.1% and 16.6%, respectively) than $R_{Sf,ex,max}$ = 0.911 (Fig. 3a). An increase in $c_{NaOH,S0}$ (from 10^{-2} kmol/m^3 to 1 kmol/m^3) had a significant positive effect on $E_{Sf,ex}$ and $E_{Rf,ex}$ (which increased from 83.87% to 96.08% and from 78.14% to 91.09%, respectively), but a negligible effect on $E_{Ef,ex}$ (93.17–94.81%) (Fig. 3b). These findings were similar to those reported in our previous study [11].

Moreover, $E_{Sf,ex}$ and $E_{Rf,ex}$ were very strongly positively correlated (r = 0.998, where r represents the Pearson correlation coefficient).

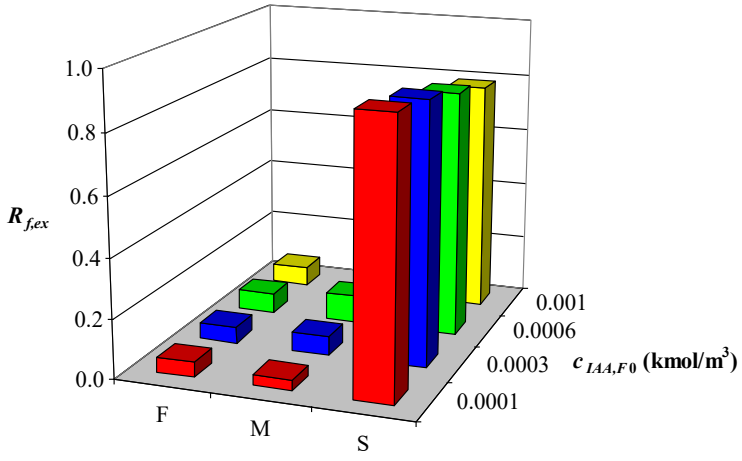

(a)

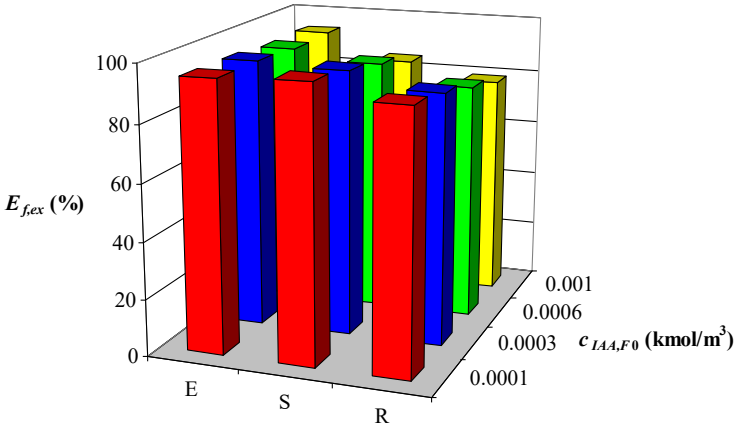

(b)

Fig. 2. Effects of initial concentration of IAA in the feed phase ($c_{IAA,F0}$) on the final values of: (a) specific amounts of IAA in the feed (F), liquid membrane (M), and stripping (S) phases; (b) extraction (E), stripping (S), and recovery (R) efficiencies of IAA ($c_{L,M0}$ = 10^{-2} kmol/m^3, $c_{NaOH,S0}$ = 1 kmol/m^3, v = 200 rpm, and t_f = 4 h).

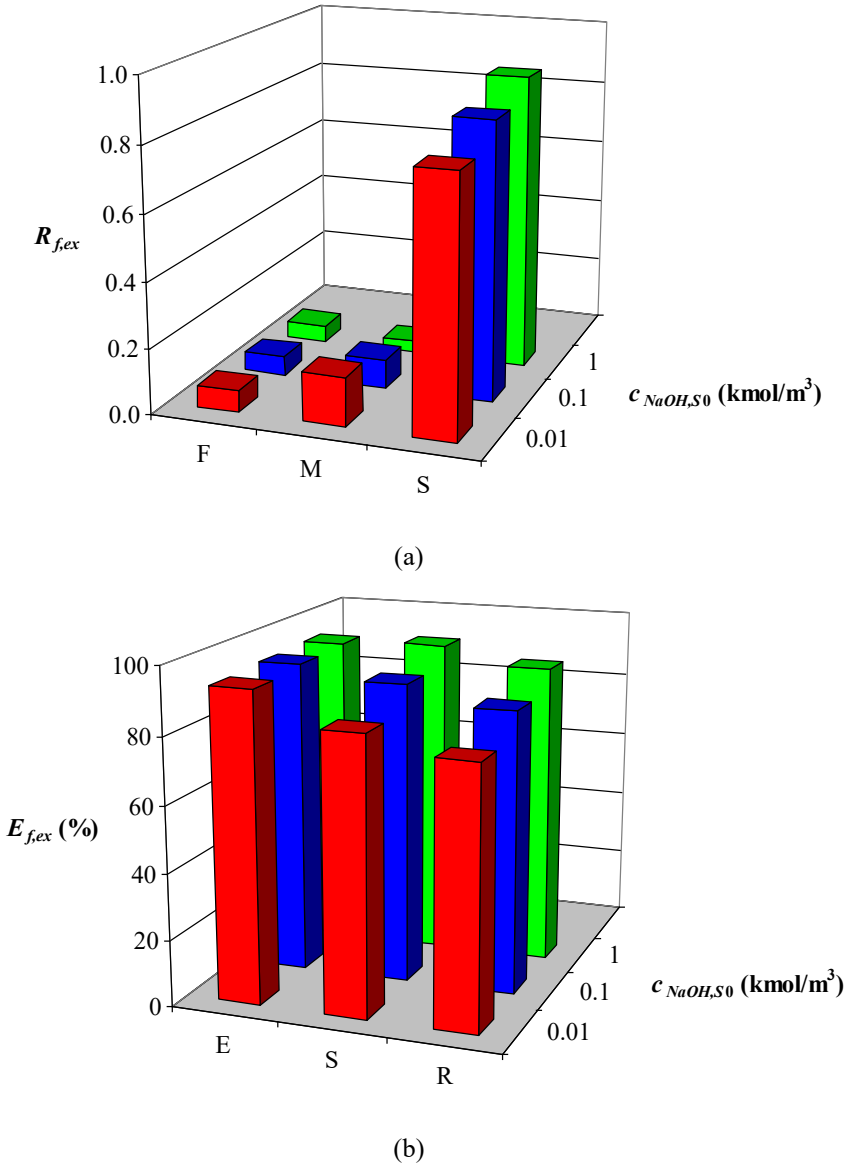

Fig. 3. Effects of initial concentration of NaOH in the stripping phase ($c_{NaOH,S0}$) on the final values of: (a) specific amounts of IAA in the feed (F), liquid membrane (M), and stripping (S) phases; (b) extraction (E), stripping (S), and recovery (R) efficiencies of IAA ($c_{IAA,F0}$ = 10^{-4} kmol/m^3, $c_{L,M0}$ = 10^{-2} kmol/m^3, v = 200 rpm, and t_f = 4 h).

5. Conclusions

Facilitated pertraction of IAA from an aqueous solution using a chloroform liquid membrane and TOA as a carrier was performed in a tube-in-tube device, where the inner tube contained the S phase (an aqueous solution of NaOH), whereas

the outer tube contained the F phase (an aqueous solution of IAA) at the top and the M phase at the bottom. Six experiments were conducted for 4 h, at 20 °C, under mechanical stirring of inner tube (v = 200 rpm), at various levels of initial molar concentrations of IAA in the F phase ($c_{IAA,F0} = 10^{-4}$–10^{-3} kmol/m^3) and NaOH in the S phase ($c_{NaOH,S0} = 10^{-2}$–1 kmol/m^3).

A kinetic model assuming consecutive irreversible first-order reactions was used to predict the specific yields of IAA in the F, M, and S phases. The adjustable parameters of the model in terms of extraction and stripping rate constants, *i.e.*, k_1 = (1.93–3.64) × 10^{-4} s^{-1} and k_2 = (2.00–4.18) × 10^{-4} s^{-1}, were obtained from experimental data. The values of k_1 and k_2 were similar, suggesting that both chemical reactions occurring at the interfaces between the F and M phases (complexation) and M and S phases (decomplexation), respectively, were rate-limiting steps. The results obtained indicated a good agreement between experimental and predicted data (R^2 = 0.948–0.998).

The maximum final value (at t_f = 4 h) of specific amount of IAA in the S phase ($R_{Sf,ex}$ = 0.911), corresponding to maximum finals values of extraction, stripping, and recovery efficiencies ($E_{Ef,ex}$ = 94.81%, $E_{Sf,ex}$ = 96.08%, and $E_{Rf,ex}$ = 91.09%), was obtained at $c_{IAA,F0} = 10^{-4}$ kmol/m^3 and $c_{NaOH,S0}$ = 1 kmol/m^3.

Acknowledgments

This work was supported by a grant from the National Program for Research of the National Association of Technical Universities – GNAC ARUT 2023 (128/04.12.2023).

REFERENCES

[1] *H. Etesami, B. R. Glick*, Bacterial indole-3-acetic acid: A key regulator for plant growth, plant-microbe interactions, and agricultural adaptive resilience, Microbiological Research, **vol. 281**, 2024, 127602.

[2] *A. Kachalkin, A. Glushakova, R.* Streletskii, Diversity of endophytic yeasts from agricultural fruits positive for phytohormone IAA production, BioTech, **vol. 11**, no. 3, 2022, 38.

[3] *C. Keswani, S. P. Singh, L. Cueto, C. García-Estrada, S. Mezaache-Aichour, T. R. Glare, R. Borriss, S. P. Singh, M. A. Blázquez, E. Sansinenea*, Auxins of microbial origin and their use in agriculture, Applied Microbiology and Biotechnology, **vol. 104**, no. 20, 2020, pp. 8549-8565.

[4] *J. B. Raval, V. N. Mehta, S. Jha, T. J. Park, S. K. Kailasa*, Synthesis of green emissive *Plectranthus scutellarioides* carbon dots for sustainable and label-free detection of phytohormone indole-3-acetic acid, Inorganic Chemistry Communications, **vol. 171**, 2025, 113660.

[5] *X. Zhang, Y. Zhou, J. Wang, X. Huang, H. S. El-Mesery, Y. Shi, Y. Zou, Z. Li, Y. Li, J. Shi, X. Zou,* Simple-easy electrochemical sensing mode assisted with integrative carbon-based gel electrolyte for in-situ monitoring of plant hormone indole acetic acid, Food Chemistry, **vol. 467**, 2025, 142342.

[6] *E. M. Myo, B. Ge, J. Ma, H. Cui, B. Liu, L. Shi, M. Jiang, K. Zhang,* Indole-3-acetic acid production by *Streptomyces fradiae* NKZ-259 and its formulation to enhance plant growth, BMC microbiology, **vol. 19**, no. 1, 2019, 155.
[7] *P. K. Sarkar, M. S. Haque, M. Abdul Karim*, Effects of GA and IAA and their frequency of application on morphology, yield 3, Pakistan Journal of Agronomy, **vol. 1**, no. 4, 2002, pp. 119-122.
[8] *Y. Liu, W. Deng, Z. Li*, Mediating effect of indole-3-acetic acid on chilling injury and fruit softening during cold storage of tomato fruit, Postharvest Biology and Technology, **vol. 230**, 2025, 113725.
[9] *Y. Feng, B. Tian, J. Xiong, G. Lin, L. Cheng, T. Zhang, B. Lin, Z. Ke, X. Li,* Exploring IAA biosynthesis and plant growth promotion mechanism for tomato root endophytes with incomplete IAA synthesis pathways, Chemical and Biological Technologies in Agriculture, **vol. 11**, no. 1, 2024, 187.
[10] *T. P. Pirog, G. O. Iutynska, N. O. Leonova, K. A. Beregova, T. A. Shevchuk*, Microbial synthesis of phytohormones, Biotechnologia Acta, **vol. 11**, no. 1, 2018, pp. 5-24.
[11] *I. Diaconu, O. C. Pârvulescu, G. I. Badea, M. Rotaru, C. Orbeci, G. Cernica*, Use of bulk liquid membranes for the removal of aspartame from aqueous media, Journal of Molecular Liquids, **vol. 409**, 2024, 125456.
[12] *I. Diaconu, O. C. Pârvulescu, S. L. Topală, T. Dobre*, Effects of process factors on performances of liquid membrane-based transfer of indole-3-acetic acid, Scientific Reports, **vol. 11**, no. 1, 2021, 23427.
[13] *A. I. Galaction, A. C. Blaga, D. Caşcaval*, Study on facilitated pertraction of folic acid in pseudosteady-state regime, Separation Science and Technology, **vol. 46**, no. 6, 2011, pp. 912-919.
[14] *A. I. Galaction, M. Poştaru, L. Kloetzer, A. C. Blaga, D. Caşcaval*, Separation of rosmarinic acid by facilitated pertraction, Food and Bioproducts Processing, **vol. 94**, 2015, pp. 621-628.
[15] *E. A. Serban, I. Diaconu, E. Ruse, G. I. Badea, A. Cuciureanu, G. Nechifor*, Evaluation of kinetic parameters at the transport of indole-3-acetic acid through bulk liquid membranes, Revista de Chimie, **vol. 68**, no. 5, 2017, pp. 903-907.
[16] *N. Baylan*, Imidazolium-based ionic liquids for acrylic acid separation from water by bulk liquid membrane and extraction methods: a comparison study, Journal of Chemical & Engineering Data, **vol. 65**, no. 6, 2020, pp. 3121-3129.
[17] *N. Baylan, S. Çehreli,* Ionic liquids as bulk liquid membranes on levulinic acid removal: A design study, Journal of Molecular Liquids*,* **vol. 266**, 2018, pp. 299-308.
[18] *N. Baylan, S. Çehreli, N. Özparlak*, Transport and separation of carboxylic acids through bulk liquid membranes containing tributylamine, Journal of Dispersion Science and Technology, **vol. 38**, no. 6, 2017, pp. 895-900.
[19] *N. Joshi, A. Keshav, A. Khapre, A. K. Poonia,* Separation of butyric acid through agitated bulk liquid membrane, Annals of the Romanian Society for Cell Biology, **vol. 25**, no. 2**,** 2021, pp. 3386-3391.
[20] *S. Tarahomi, G. H. Rounaghi, H. Eshghi, L. Daneshvar, M. Chamsaz,* Selective transport of silver (I) cation across a bulk liquid membrane containing bis-β-enamino ester as ion carrier, Journal of the Brazilian Chemical Society*,* **vol. 28**, 2017, pp. 68-75.